
Oct 23rd, 12:00 AM

Experimental Study on the Lateral Buckling Behaviour of Cold-formed Beams

Venkatakrishnan Kalyanaraman

A. C.R. Djugash

Follow this and additional works at: <https://scholarsmine.mst.edu/isccss>



Part of the [Structural Engineering Commons](#)

Recommended Citation

Kalyanaraman, Venkatakrishnan and Djugash, A. C.R., "Experimental Study on the Lateral Buckling Behaviour of Cold-formed Beams" (1990). *International Specialty Conference on Cold-Formed Steel Structures*. 2.

<https://scholarsmine.mst.edu/isccss/10iccfss/10iccfss-session4/2>

This Article - Conference proceedings is brought to you for free and open access by Scholars' Mine. It has been accepted for inclusion in International Specialty Conference on Cold-Formed Steel Structures by an authorized administrator of Scholars' Mine. This work is protected by U. S. Copyright Law. Unauthorized use including reproduction for redistribution requires the permission of the copyright holder. For more information, please contact scholarsmine@mst.edu.

**EXPERIMENTAL STUDY ON THE
LATERAL BUCKLING BEHAVIOUR OF COLD-FORMED BEAMS**

by

**A.C.R.DJUGASH*
V.KALYANARAMAN****

ABSTRACT

Experimental investigations conducted on the lateral buckling behaviour and ultimate load carrying capacity of cold rolled thin-walled sigma and Z section beam specimens are reported. The behaviour of the laterally unrestrained beam specimens subjected to two point loading are studied with reference to their midspan deflections and maximum moment section strains. The experimental failure loads compare well with the results of a computer program NISAT.

INTRODUCTION

Thin walled cold-formed beams of open cross-sections are used extensively in practice, since they constitute an economical use of material in providing the necessary stiffness and strength for lightly loaded structures. Thin walled beams of symmetrical or unsymmetrical sections, which are designed to eliminate the elastic local buckling before failure, when subjected to bending about the major principal axis, are prone to fail in flexural yielding or flexural-torsional buckling mode.

The earliest reported tests conducted on laterally unrestrained beams of channel and Z-section were by Hill [1954]. He tested four channel sections and four Z-sections to study the lateral buckling behaviour and suggested simple expressions to calculate the buckling load. After the tests by Hill, no such beam tests have been done with the aim of understanding the behaviour in lateral bending and lateral torsional buckling modes of laterally unrestrained thin walled beams. The behaviour of thin walled beams for various load positions with respect to their shear centre location has not been experimentally studied by any one. The procedure and results of tests conducted on laterally unrestrained cold formed beams of Sigma and Z-sections are reported in this paper. The behaviour of thin walled beams even into the geometric nonlinear range upto failure for various points of application of the load with respect to the shear centre, reported in this paper, have not been studied so far by anyone else.

* ASSISTANT DIRECTOR, Structural Engineering Research Centre,
Taramani, Madras 600 113, INDIA.

** PROFESSOR, Department of Civil Engineering,
Indian Institute of Technology, Madras 600 036,INDIA.

TEST SET-UP

The test set-up consists of supporting frames, cross rafters and cleat supports. The transverse support frames were fixed apart on a structural floor to the required span length. The cross rafters in the support frame may be arranged either flat or at any desired slope as shown in Figs. 1(a) and 1(b). With the provision to alter the slope it was possible to align the principal axis of the Sections at any angle to the gravity axis. The cross rafters were quite rigid and were pin connected to the frames, which in turn were rigidly fixed to the structural testing floor. The test specimen was supported on the two cross rafters, using the cleat supports normally used in practice (Fig.2).

Two point loading was chosen to have a constant moment region, so as to measure the strain and deflections at the centre of the beam without being affected by the local effects of the load. The two concentrated loads were applied at one fourth of the span length, away from each end support of the test beams, so that the bending moment, shear force, and deflection closely matched with the values corresponding to the uniformly loaded simply supported beams.

The loads were applied by means of a pair of special loading devices which are as shown in Fig.3. The loading device consisted of a 12 mm thick circular disc, with a suitable central cut-out to accommodate the test specimen passing through it. A steel wire rope passed in the groove provided within the thickness around the perimeter of the disc and around a pulley at the bottom, from which a loading pan was hung using chain links. The load placed in the loading pan was transferred from the rope to the disc through the periphery of the disc, by radial pressure. The loading device caused the resultant of the applied load to always pass through the centre point of the circular disc, in the direction of gravity.

The test specimen was marked for the location of the support cleat bolt holes. The load point disc attachment bolt holes were marked depending upon the point of application of the load over the cross section, appropriately. The holes were drilled accordingly. The actual cross sectional dimensions of the beam were measured using a vernier caliper and a screw gauge at a few locations along the span length to get the average dimensions. The initial imperfection such as lateral bend, twist, etc., if any, was also measured. The electric resistance strain gauges were then fixed at the midspan sections of the beam.

The loading devices were inserted along with the steel wire rope from the ends of the test beam and fixed firmly to the specimen. The loading devices were aligned accurately before tightening the fasteners, so that the desired point of application of the load over the cross section coincides with the centre of the disc. Subsequently, the test specimen was placed over the rafters and the cleat bolts connecting the specimen to the cleat supports were tightened. The dial gauges were connected at the midspan.

TEST SPECIMEN

Three sigma sections and one Z section were chosen for studying the behaviour due to load applied through the principal axis caused lateral buckling failure. As the sigma sections are monosymmetrical sections, they were held by rafters set flat so that the points of application of the loads were always parallel to the web and the minor principal axis. The three points of application of the loads in the sigma section tests were (i) at the shear centre (SC), (ii) at the point of intersection of the top flange with the line parallel to the web passing through shear centre (TF), and (iii) at the point of intersection of the bottom flange with the line parallel to the web passing through shear centre (BF). The points of application of the loads are shown in Fig.4.

The Z section specimen was held at the support in a way by rafters such that the minor principal axis more or less coincided with the gravity axis, causing uniaxial bending about the major axis due to the gravity load (SL/SC). The specimen named as Z4 was loaded through the shear centre. The measured dimensions of the test specimens are given in Table 1. All the specimens had sufficiently stocky plate elements, precluding elastic local buckling.

INSTRUMENTATION

The vertical and horizontal deflections at the midspan of the beam were measured with the help of circular type dial gauges. The least count of the dial gauge was 0.1 mm. Four circular type dial gauges were used to measure the vertical and horizontal displacements of the top flange-web junction and bottom flange-web junction. Using these readings, it is possible to calculate the centre span horizontal and vertical displacements at the shear centre as well as the torsional rotation of the section.

The electrical resistance strain gauges, 20 mm long, were used for the strain measurement. At the centre span of each specimen, the strain gauges were attached, oriented along the length, adjacent to all the junctions of the plate elements of the cross section on one side of the thickness, in order to obtain the normal stress distribution over the cross section. Fourteen such gauges were used for the Sigma section specimens and ten for the Z section specimen. The details of the exact location of the strain gauges have been given by Djugash [1988].

TESTING PROCEDURE

The dial and strain gauge readings were initialised for the condition of self-weight plus the weight of the circular loading devices. The loading pans were then suspended to hang from the pulley at the bottom of the wire loop passing over the disc. Loads of 50 or 100 Neutons were added simultaneously on the two pans in a balanced manner. The strain and deflection measurements were recorded after every loading stage, until the specimen failed. Ultimate failure loads were also recorded. The test specimen S1 after its failure is shown in Fig.5.

EVALUATION OF TEST RESULTS

Sigma Specimen S1-Loaded through the Shear Centre

The sigma sections are symmetric about the major axis. Specimen S1 was loaded parallel to minor axis through the shear centre. The initial lateral midspan imperfection, measured in the specimen, was around 4.5 mm.

The load deformation diagram of the specimen S1 is given in Fig. 6(a). Although the gravity load should not cause any horizontal displacement, the beam experienced a small horizontal displacement even from the first load increment, which was due to the initial imperfection. As the imperfection was in the positive y-direction (Fig.6a), the beam also deflected towards the positive direction. The beam load versus vertical deflection behaviour was linear essentially upto about 1.2 kN. The twisting deformation, which was negligible earlier, was also linear up to that load. Beyond 1.2 kN load, the lateral deflection increased at a faster rate, although the twisting increased at a higher rate only after a load of about 1.6 kN. Above 1.8 kN, the load deformation behaviour showed distinct stiffening effect, possibly due to the axial shortening restraint provided by the supports.

The load versus strain diagrams given in Fig.6(b) also indicate essentially a linear range up to about 1.2 kN beyond which the behaviour becomes nonlinear. Although the section should theoretically experience uniform compression and uniform tension over the entire top and bottom flanges, respectively, the maximum compression was at the top flange-web junction and the tension at the bottom flange-lip junction. This was due to the positive horizontal displacement and twisting, particularly in the nonlinear range. This strain gradient in flange, reducing the compression at the top flange-lip junction, has helped the section to carry higher load by avoiding the lip failure, even when the maximum compressive strain at web-flange junction reached the yield strain.

The failure occurred when the total load at each of the load point, including the weight of the loading devices, reached 1.93 kN. The failure was accompanied by dramatic increase in the transverse displacement. At failure, a local wrinkle at the top flange-web junction, where the maximum compression occurred, was observed at the midspan of the beam.

Sigma Specimen S2 - Loaded at the Top Flange

In this test also the load was parallel to the web. However, the point of application of the load was set to pass through the intersection of the top flange with the minor principal axis passing through the shear centre. The initial horizontal imperfection measured in specimen S2 was about 7.0 mm.

The variation of deflections of the specimen with loading is shown in Fig.7(a). The initial load deformation behaviour of S2 was similar to that of S1, linear up to around 1.0 kN. The shear span

of S2 was 1050 mm, unlike the shear span of 1125 mm for all other sigma sections. The destabilising effect of the top flange loading may be observed in the relatively larger twisting deformations of the specimen S2 compared to that of S1 for the same load. Similar to the specimen S1, in the advanced nonlinear range, the load deformation behaviour showed distinct stiffening effect.

The load versus strain diagrams of S2, given in Fig.7(b), are also almost similar to those of S1 in the linear range of up to around 1.0 kN beyond which they became highly nonlinear. The maximum compressive strain was at the junction of the top flange and web. Although the top flange-lip junction experienced compression at the linear load levels, the strain became tensile when the load reached nonlinear range. The strain gradient observed in the top flange helped the beam to withstand load higher than even the load causing the local yielding at top web-flange junction, by avoiding the premature lip failure under high compressive stress.

The failure occurred when the total load at each load point reached 1.89 kN including that of the loading devices. The failure occurred with the top flange-web junction experiencing crippling. Even after the local yielding in tension and compression, the specimen carried loads further aided by the strain gradients in the elements. However, the failure load was less than that obtained from the shear centre loading case.

Sigma Specimen S4 - Loaded through the Bottom Flange

The specimen S4 was also loaded parallel to minor principal axis. However, the point of application of the load was set to pass through the intersection of the bottom flange with the minor principal axis line and passing through the shear centre.

The load deformation behaviour is shown in Fig.8(a). The beam was having a negative initial lateral mid span imperfection of 5.0 mm. This induced the beam to deflect towards the negative direction (towards the shear centre). The vertical displacement was almost linear till the failure load. The horizontal displacement became slightly nonlinear beyond 0.8 kN load upto which it was negligible. The stabilising effect due to the torque caused by the bottom flange loading resulted in considerable reduction in the twist of the beam S4 until almost the failure load was reached. The load versus strain diagrams are shown in Fig. 8(b). The behaviour was that of a typical beam subjected to the major axis bending. Due to the symmetric bending, the entire cross section above the major axis experienced compression and below the major axis experienced tension. The largest compressive and tensile strain were at the extreme fibres away from the major axis, namely, top flange and bottom flange, respectively. Once the beam entered into the nonlinear range, due to the twisting deformation and the lateral displacement, the maximum tensile strain occurred at the bottom flange-web junction and the maximum compressive strain at the top flange-lip junction. The maximum compressive stress was the largest stress due to the combined vertical and horizontal bending stresses and the warping stress, remained below yield stress even close to failure load.

The displacement and strain readings were taken up to the total load of 1.58 kN at each loading point. The failure occurred suddenly at 1.58 kN before the next load increment and was essentially a lateral buckling type of failure. Due to the horizontal displacement and the consequent large compressive strain at the top flange-lip junction, the lip local buckling triggered the failure.

Z-Section Specimen - on Slope and Loaded through the Shear Centre

The specimen Z4 was loaded through the shear centre, but the loading was not parallel to the web. The beam was placed on a slope of 1 in 3 (18.43°) and the principal axes of the Z-section (inclined at 19.55° to the web) was more or less aligned with the gravity (loading) axis. Therefore, the load was virtually acting along the minor principal axis and the behaviour of the beam was similar to the case of the uniaxial bending about the major axis.

Fig.9(a) shows the load deformation behaviour of Z4. The vertical displacement was essentially linear until up to the last reading taken prior to the failure. The twisting deformation was also linear up to two-third of the failure load and thereafter both horizontal deflection and twisting were slightly nonlinear. The lateral and torsion deformations were quite small comparatively until close to failure load and increased considerably only at the last loading stage. The load deformation behaviour was typical of the major axis bending cases, which fail by the lateral buckling. The increase in v and ϕ from the very first load indicated small minor axis bending and twisting.

The strain versus load diagrams are shown in Fig.9(b). Due to almost symmetric bending, the entire cross section above the major axis experienced compression and below the major axis experienced tension. The largest compressive and tensile strain were at the extreme fibres away from the major axis, namely the top flange-lip junction and the bottom flange-lip junction. The load versus strain diagram indicates essentially a linear behaviour over a major loading range with a sudden increase in the extreme fibre tensile and compressive strains closer to the ultimate load.

The failure occurred suddenly when the concentrated load at each loading point was 2.45 kN and was essentially a lateral buckling type of failure. Due to large lateral displacement, and the consequent large compressive strain at the top flange-lip junction, the lip buckling was observed at failure (Fig.10).

DISCUSSION:

Sigma specimens S1, S2 and S4 loaded to cause bending about major axis, exhibited almost linear load deformation behaviour upto the theoretical buckling load. The transverse deflection and rotation were also small until this load. The specimen S4 failed immediately after the lateral buckling load. Whereas the specimen S1 and S2 exhibited additional strength beyond lateral buckling load before failure. This additional strength depends upon plastic strain capability of maximum

compression region. Specimen Z4 also failed immediately after the lateral buckling load similar to specimen S4, essentially in lateral buckling mode.

The ultimate failure of all the specimens, including the weight of loading devices is given in Table-2. The experimental results are compared with the analytical results obtained from a computer program for Nonlinear Instability Analysis of Thin Wall Members by Djugash [1990]. The analytical results are presented under two sub-heads, one corresponding to linear instability analysis and the other corresponding to nonlinear instability analysis. It can be seen that the linear instability loads are always conservative compared to the experimental results, whereas the nonlinear instability analysis results are closer to the experimental failure loads. It is also seen in Figs. 6 to 9 that beyond the theoretical linear buckling load only the large transverse deformation, twisting and increase in stress (high nonlinearity) are exhibited in the experimental results. The difference between the linear and nonlinear analysis results is due to the strain gradient in the flanges and the large deformation effects.

CONCLUSION

Experimental investigation is a necessity in any study on structural behaviour, even if it is only to calibrate some analytical procedure. In this paper the details of an experimental investigation on the lateral buckling behaviour of thin walled cold-formed member is presented. Cold-formed beams loaded along the principal axis exhibit linear behaviour over a large range of loading upto lateral buckling load. However, they exhibit a nonlinear behaviour in the post-buckling range which need not be negligible. The lateral displacement and the consequent twisting deformation cause the nonlinearity before failure. Post-buckling strength, however, depends upon the ability to sustain plastic strain at the extreme compression fibre until partial plastification of the cross section and large deformation effects.

APPENDIX.--REFERENCES

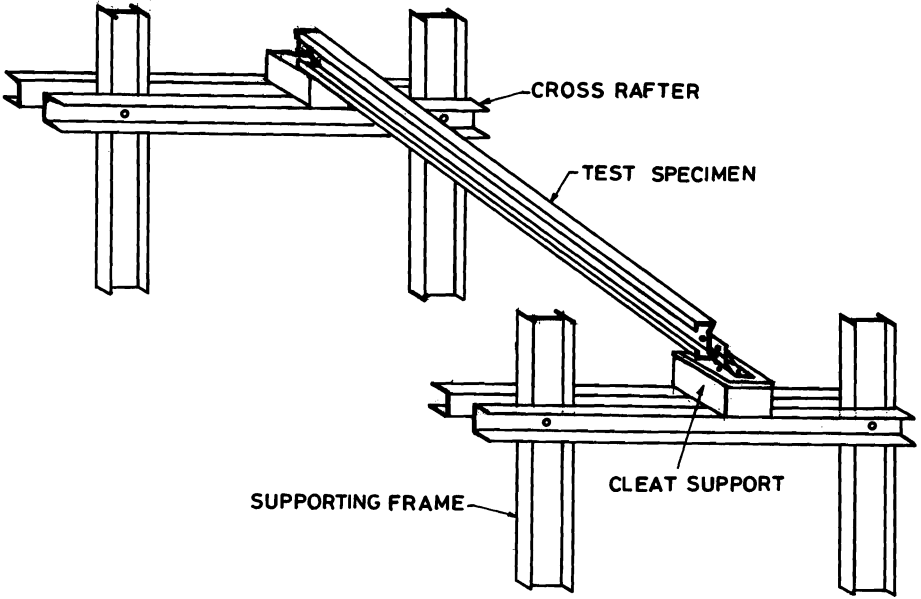
1. Djugash, A.C.R., "Nonlinear Biaxial Bending Behaviour of Thin Walled Members", Thesis submitted for the fulfillment of the degree of Doctor of Philosophy in Civil Engineering, Indian Institute of Technology, Madras, March 1988, pages 293.
2. Djugash, A.C.R., and Kalyanaraman, V., "Nonlinear and Instability Analysis of Thin Walled Members", Proceedings of the National Symposium on 'Advances in Steel Structures', Feb.7-9, 1990, IIT, Madras, Ed. V.Kalyanaraman, Tata Mc Graw-Hill Pub.Co.,Ltd., pp 105-114
3. Hill, H.N., "Lateral Buckling of Channels and Z Beams", Transactions of the ASCE, Vol.119, 1954, pp.829-841.

TABLE 1: Dimensions of specimens

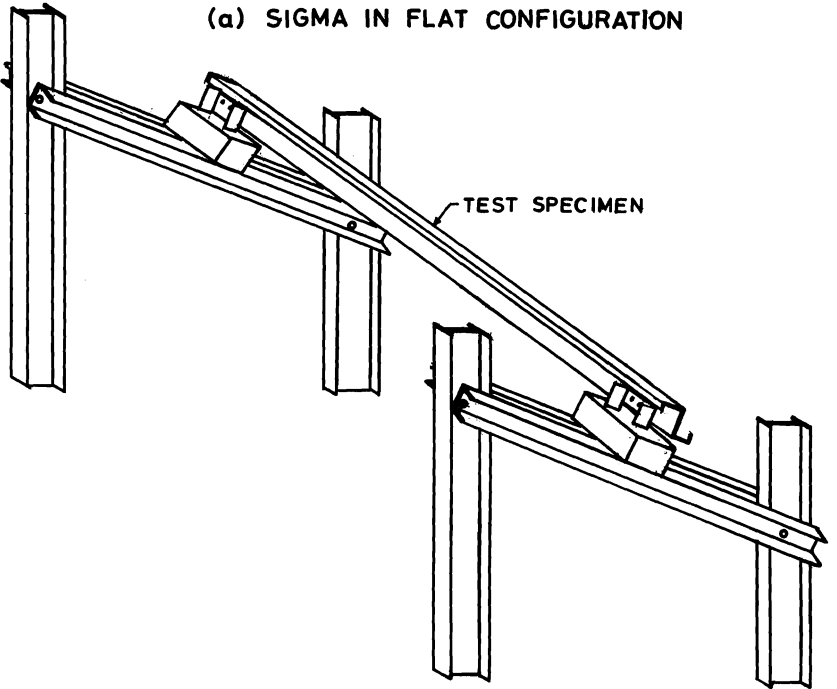
Sl. No.	Beam Code	Designation	Loading condition	L1 (mm)	B1 (mm)	D (mm)	B2 (mm)	L2 (mm)	T (mm)
(1)	(2)	(3)	(4)	(5)	(6)	(7)	(8)	(9)	(10)
1	S1	140x50x2	SC	14.5	51.2	140.1	51.0	17.0	2.03
2	S2	140x50x2	TF	16.2	51.0	140.4	50.4	14.7	2.04
3	S4	140x50x2	BF	14.5	51.0	140.1	50.8	16.0	2.19
4	Z4	150 200	SL/SC	15.3	58.2	150.0	53.3	19.2	1.95

TABLE 2: Failure load of test specimens

Sl. No.	Beam Code	Loading condition	Clear span (mm)	Shear span (mm)	Failure load P (kN) at each load point		
					Experimental	NISAT Analysis	
(1)	(2)	(3)	(4)	(5)	(6)	Linear Instability	Nonlinear Instability
						(7)	(8)
1	S1	SC	4500	1125	1.93	1.20	1.61
2	S2	TF	4500	1050	1.83	1.00	1.72
3	S4	BF	4500	1125	1.58	1.54	1.63
4	Z4	SL/SC	4500	1125	2.45	2.44	2.44

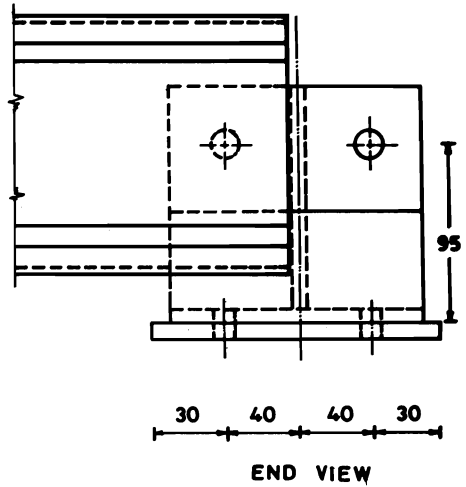
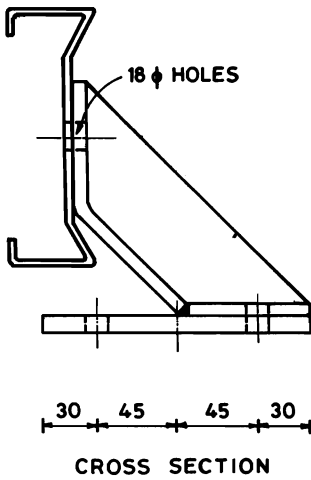


(a) SIGMA IN FLAT CONFIGURATION



(b) Z - BEAM IN SLOPED CONFIGURATION

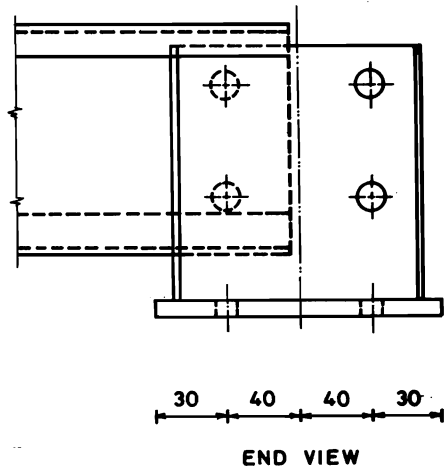
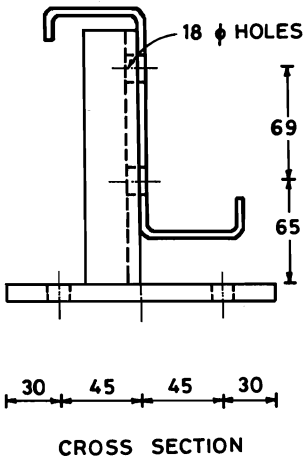
FIG.1 SUPPORTING FRAME



(a) SIGMA BEAM

NOTE :

ALL DIMENSIONS ARE IN mm.



(b) Z-BEAM

FIG. 2 SUPPORT CLEAT CONNECTION DETAILS

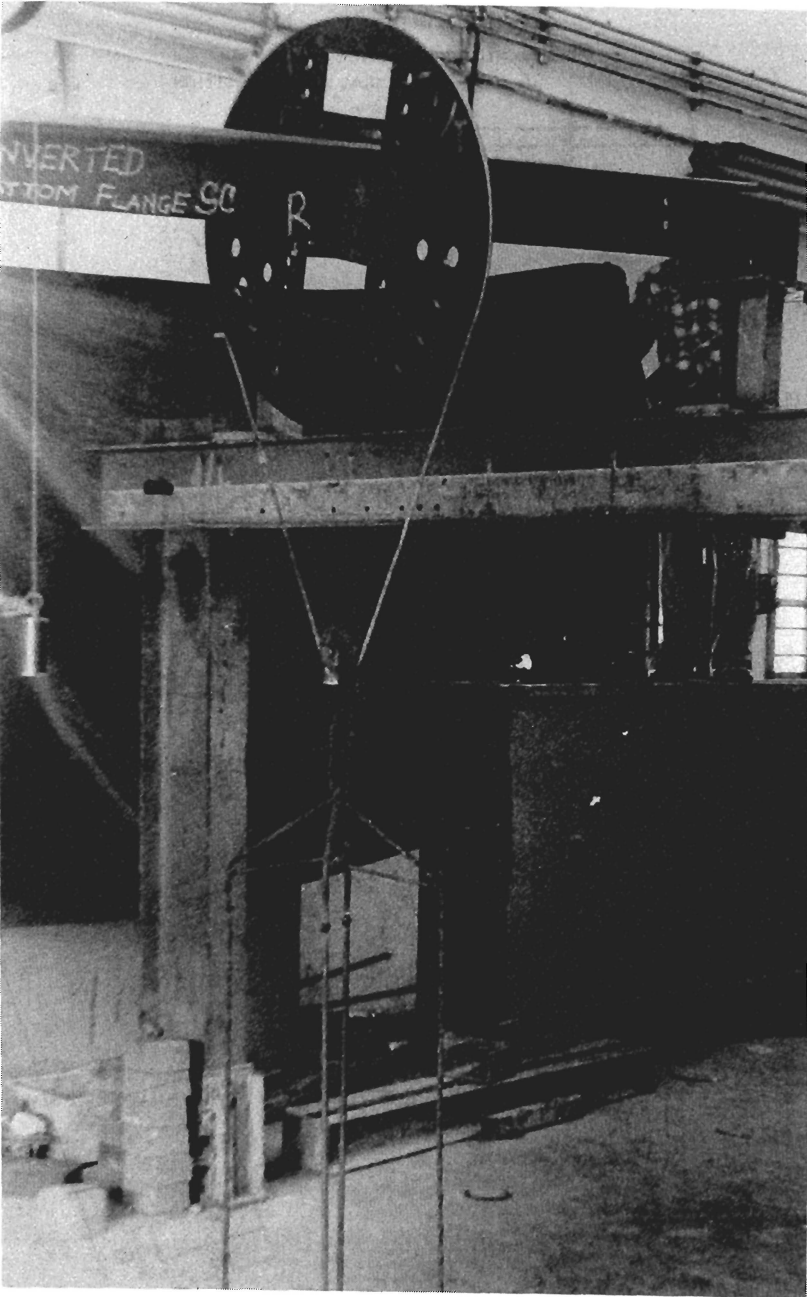
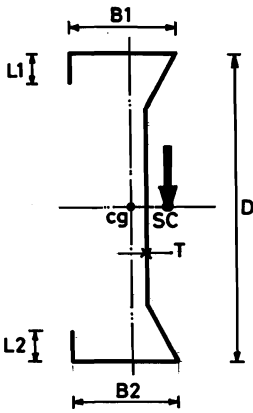
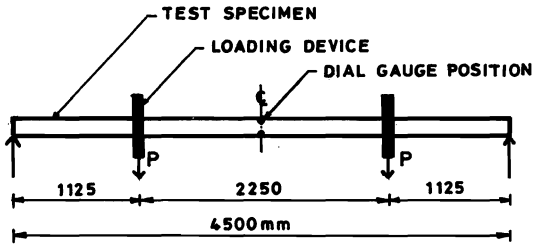
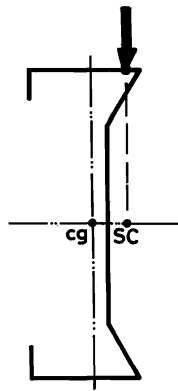


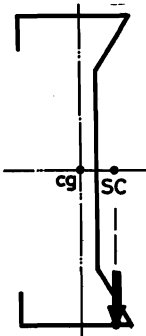
FIG. 3 SPECIAL LOADING DEVICE



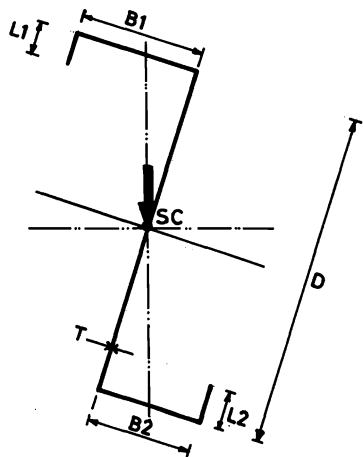
SHEAR CENTRE LOADING-S1



TOP FLANGE LOADING-S2



BOTTOM FLANGE LOADING-S4



SHEAR CENTRE LOADING ON SLOPE-Z4

FIG.4 TEST SPECIMENS

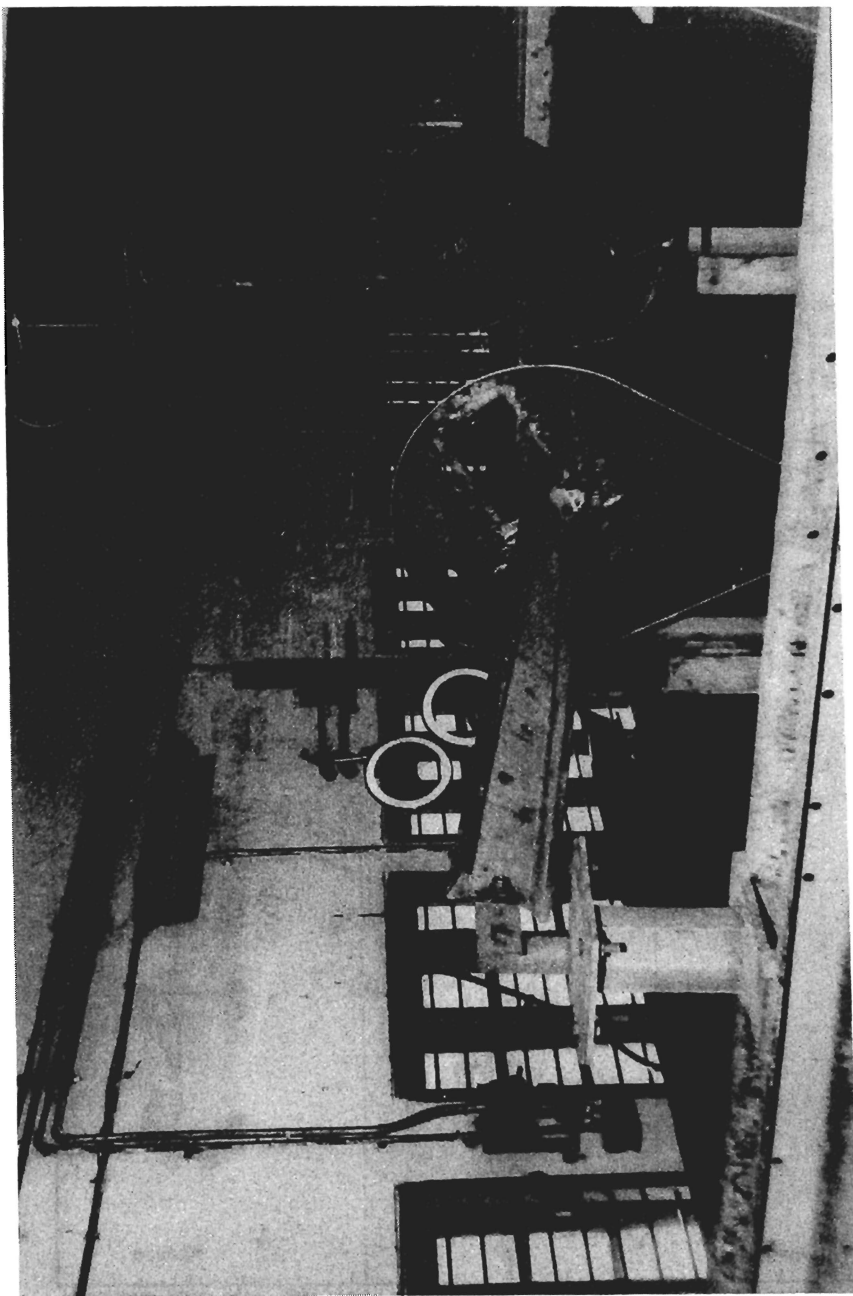
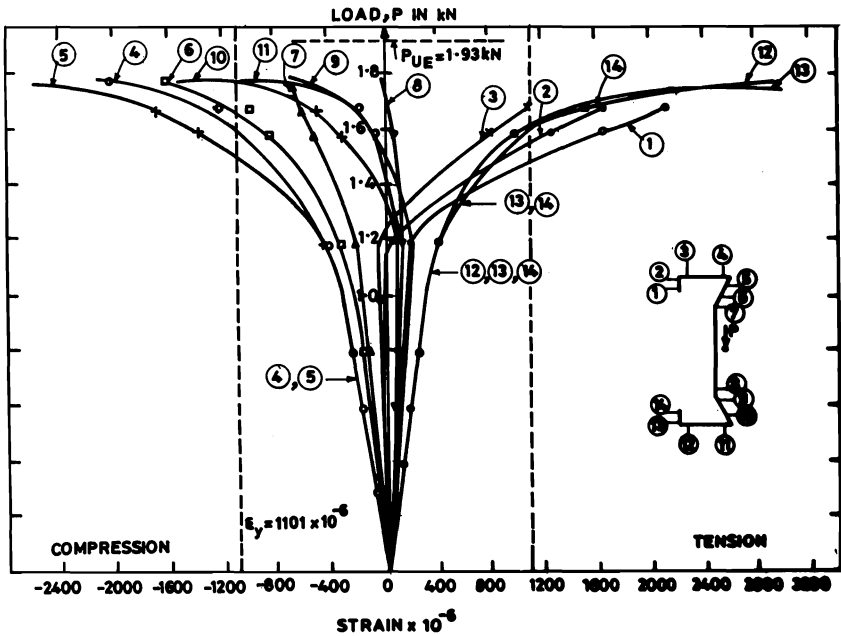
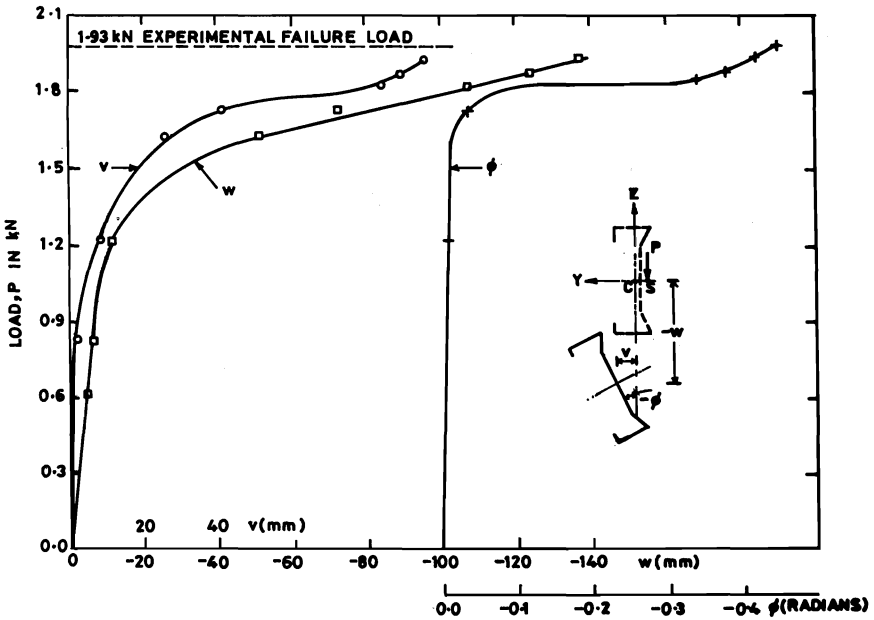


FIG. 5 TEST ON SIGMA BEAM -S1



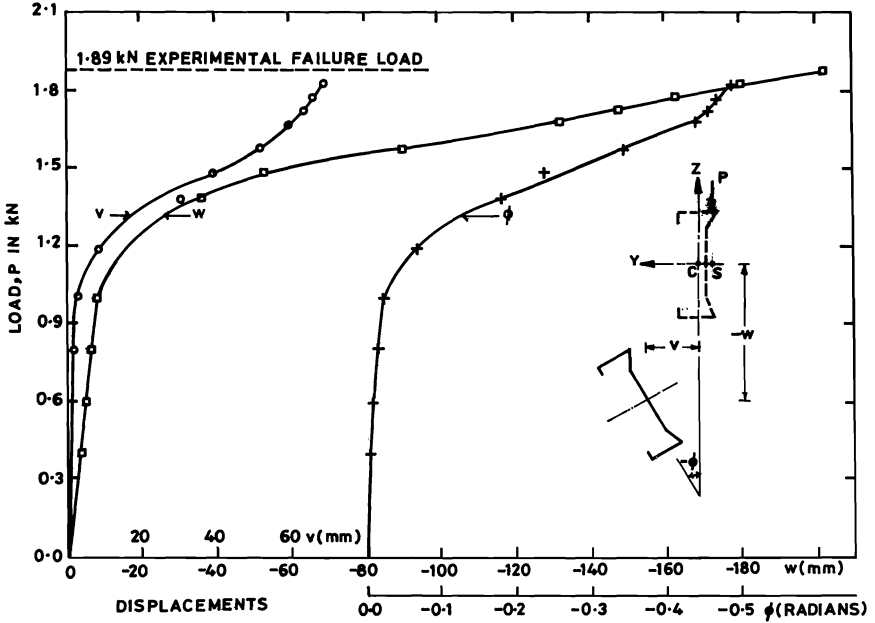


FIG.7a MIDSPAN DISPLACEMENTS IN S2

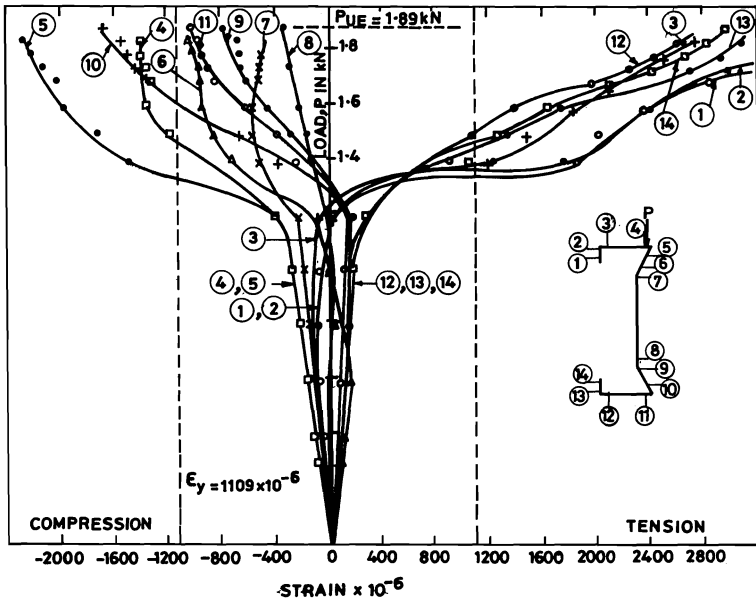


FIG.7b MIDSPAN LONGITUDINAL STRAINS IN S2

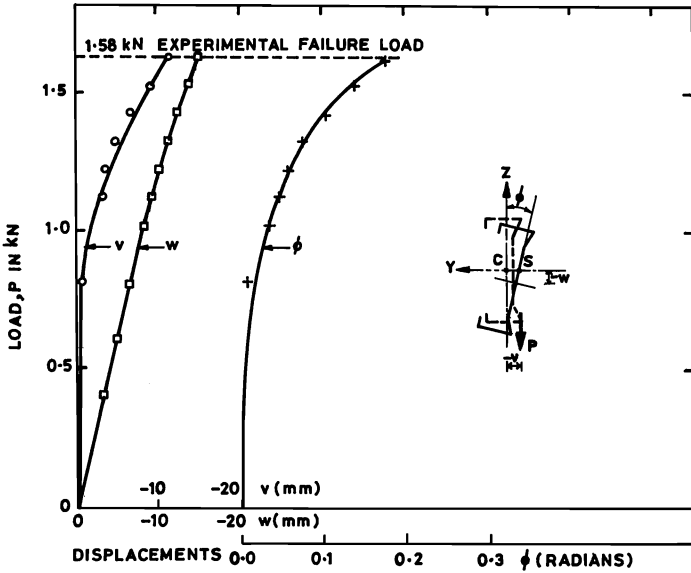


FIG. 8a MIDSPAN DISPLACEMENTS IN S4

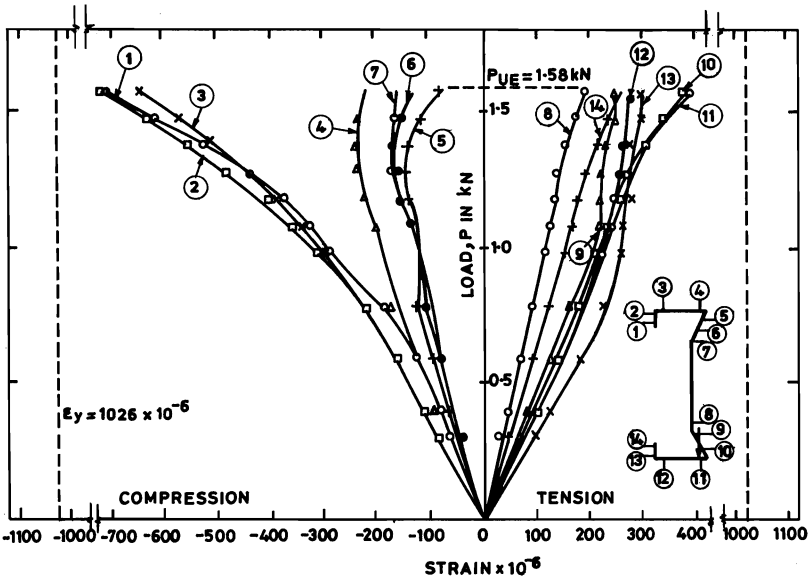


FIG. 8b MIDSPAN LONGITUDINAL STRAINS IN S4

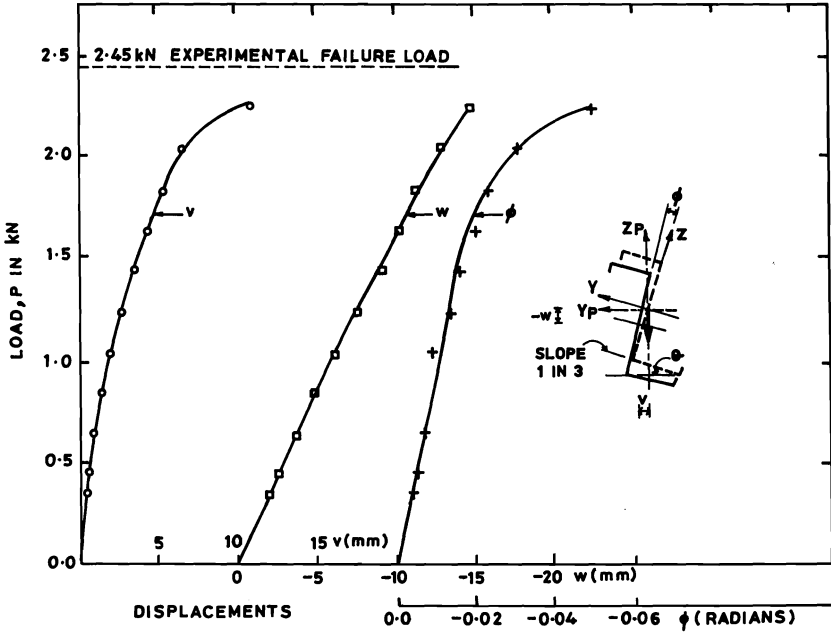


FIG. 9a MIDSPAN DISPLACEMENTS IN Z4

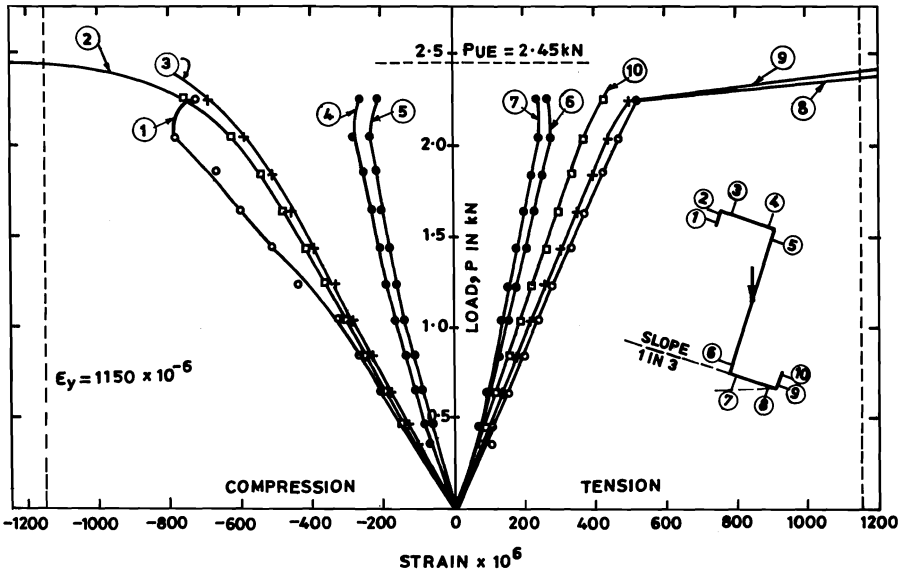


FIG. 9b MIDSPAN LONGITUDINAL STRAINS IN Z4

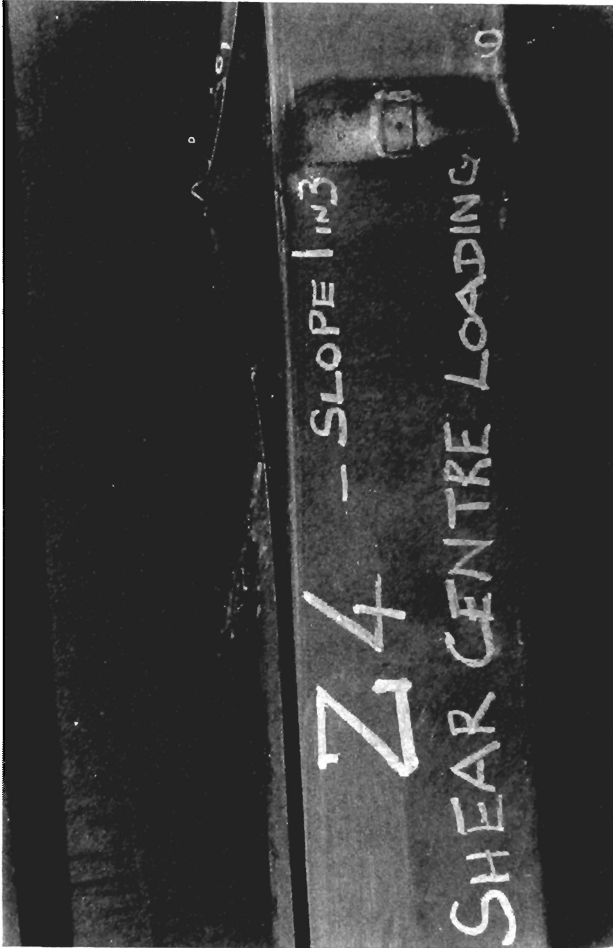


FIG. 10 BUCKLING FAILURE OF SPECIMEN Z4